Chapter

Return Stroke Process Simulation Using TCS Model

Fridolin Heidler

Abstract

The Traveling Current Source (TCS) model describes the electrical processes during the lightning return stroke phase. The TCS model assumes that the lightning current is injected at the top of the increasing return stroke channel represented by a transmission line. The electric and magnetic field is calculated based on the spatial and temporal distribution of the lightning current along the return stroke channel. It is shown that the main characteristics of the measured electric and magnetic fields can be reproduced with the TCS model. These are the Initial Peak of the electric and magnetic fields for near intermediate and far distances, the Ramp (up to the maximum) of the near electric field, the Hump of the near magnetic field after the initial peak, and the Zero Crossing of the far distant electric and magnetic fields. The fundamentals of the model are presented, and the model is extended to consider the current reflections occurring at the ground and the upper end of the return stroke channel. To this end, the ground reflection factor ρ and the top reflection factor R are introduced. Due to the increasing return stroke channel, the top reflection factor is a function of the return stroke velocity. The total current is composed of the source current according to the TCS model and the reflected currents. It is shown that the ground reflection causes significant variation in the waveform of the channel-base current and the electric and magnetic fields.

Keywords: Return Stroke, Lightning, Electric Field, Magnetic Field, Simulation, TCS model, Ground Reflection, Channel Top Reflection

1. Introduction

The threat of lightning can be classified into two separate groups, given by the direct and the indirect effects. The direct effects include physical losses due to the hot lightning channel and the high lightning current. Typical direct effects are mechanical damage, fire ignition, and the life-threatening hazard by lightning impact to persons. The basic protection measures against this threat are installing air termination systems, down conductor systems, and grounding systems [1, 2].

In contrast, the indirect effects are caused by nearby lightning events. Typical indirect effects are over-voltages which affect the electric and electronic systems and devices. The over-voltages are caused by partial currents that enter the structure and the coupling effects due to the high electric and magnetic fields radiated by lightning.

Meanwhile, the economic losses caused by the indirect effects are much higher compared to the direct effects [3]. This is attributed to the widespread use of electrical and electronic systems and devices in private buildings and industrial

facilities. Countermeasures require the integration of lightning protection into the rules of electromagnetic compatibility (EMC) [4].

The lightning current may contain several components, from which the so-called return stroke current represents the highest threat. The return stroke current is a short current pulse, which lasts some tens to some hundreds of microseconds and may have an amplitude up to more than 100 kA (For example, see [5]). The currents generate electric and magnetic fields, which may be so intense that they couple over-voltages of several kilo-volts into installations inside buildings.

Examining these over-voltages requires simulation models that consider the return stroke process, including the electric and magnetic fields. To this end, return stroke models were developed which calculate the electric and magnetic field from the spatial and temporal distribution of the lightning current along the return stroke channel [6–10]. In these models, current reflections at the ground are commonly ignored. For this reason, the so-called traveling current (TCS)-model [11, 12] was developed, which considers the current reflections at the striking point.

One key task of the EMC is to evaluate the maximum threat which the electrical equipment and systems have to withstand. In the case of lightning, the electric and magnetic fields are highest if the orientation of the lightning channel is perpendicular to the earth's surface. For this reason, the lightning channel is considered with vertical orientation.

2. Physical background on TCS model

Most of the observed cloud-to-earth flashes are of negative polarity. For this reason, the TCS model is presented for the negative return stroke. The return stroke phase involves two periods, the initial connecting leader period, followed by the second period when the downward leader channel is discharged.

2.1 Connecting leader period

The negative cloud-to-ground lightning starts with processes in which charges are separated and rearranged inside the thundercloud. Due to these processes, negative charges are accumulated, and the center of the negative charge is built up in the lower part of the thundercloud. When the accumulated charge exceeds a critical value, a negative leader is formed, propagating from the negative charge center towards the ground.

The hot core of the leader is surrounded by negative charges, which also move down. When the downward propagating leader comes close to the ground, the electric field increases due to the charge approach. Then, a connecting leader starts from the ground as soon as the electric field exceeds a critical value.

The electric field at the tip of the connecting leader is so high that charge carriers are separated by impact and photoionization around the leader tip. The electric field accelerates the charge carriers, and they move to the tip of the connecting leader. In this way, a current is injected at the tip of the connecting leader, shown in **Figure 1a**. The injected current is given by:

$$i(h) = \int_A \vec{j}\, d\vec{A}, \text{ with } \vec{j} = Q''' \cdot b \cdot \vec{E} \tag{1}$$

Q''': Charge density of the charge carriers.
b: Electrical mobility of the charge carriers.
E: Electric field.

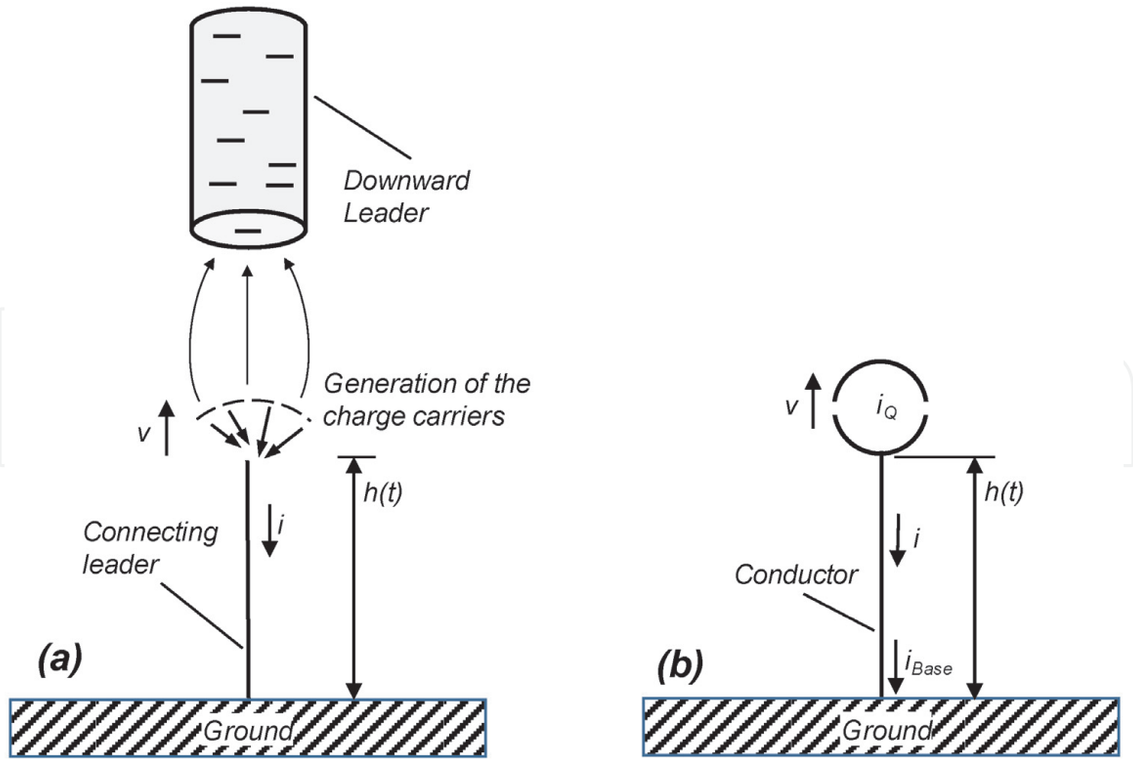

Figure 1.
Assumption for the connecting leader period, showing (a) the physical model and (b) the electrical equivalent circuit.

j: Current density.
h: Height of the upper end of the connecting leader.

In the equivalent circuit, the current injection can be represented by a current source $i_Q = i\ (h)$ located at the tip of the connecting leader in the height h. The current source travels at the connecting leader's upper end, which increases with the velocity v, shown in **Figure 1b**.

A certain time period is needed to separate the charge carriers and for the thermal ionization process at the tip of the connecting leader. For this reason, the traveling velocity (v) is less than the speed of light (c). On the other hand, the lower section of the connecting leader is already ionized, and this section represents a more or less good electrical conductor. Therefore, it is assumed that injected current propagates from the connecting leader tip with the speed of light to the ground.

2.2 Discharge process of downward leader channel

After contacting the upward propagating connecting leader with the downward leader, the negatively-charged shell of the downward leader is discharged, shown in **Figure 2a**. The charge carriers stored in the volume dV are injected into the tip of the lightning channel at the height h during the time interval dt. The current is given by:

$$i(h) = \frac{dQ}{dt} = \int_V \frac{dQ'''}{dt} dV \tag{2}$$

Also, in this case, the current injection can be represented by a current source $i_Q = i(h)$ located at the tip of the increasing return stroke channel. **Figure 2b** shows the electrical equivalent circuit with the current source, which travels at the tip of the increasing return stroke channel towards the thundercloud.

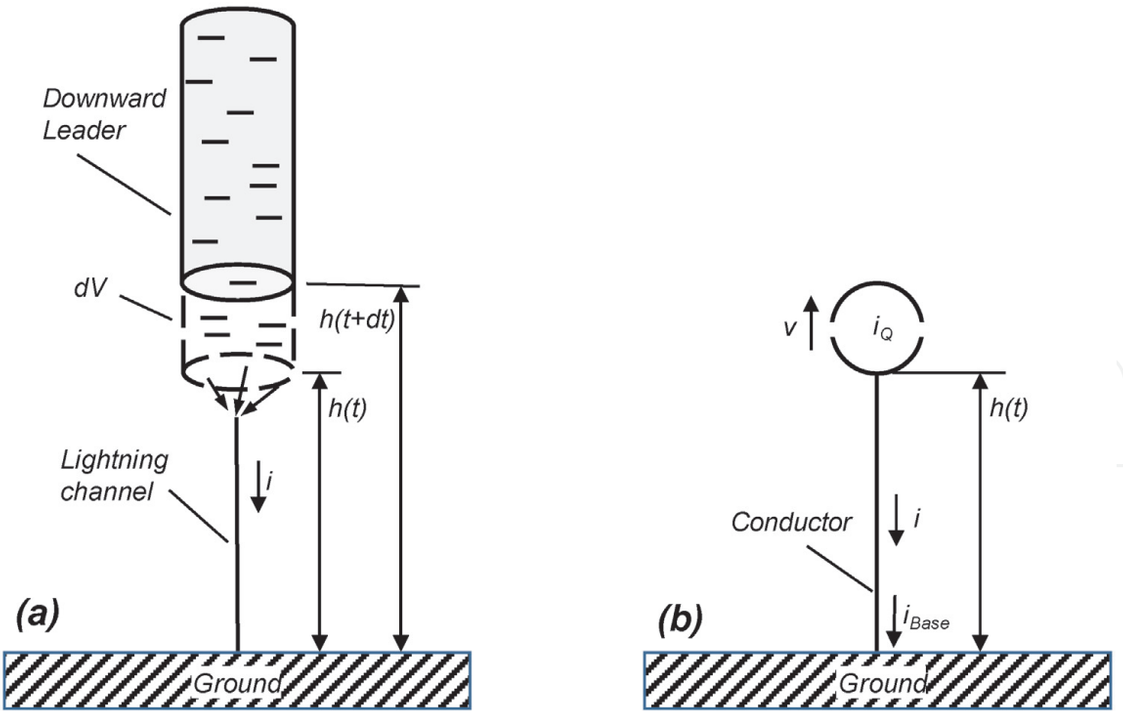

Figure 2.
Assumption for the discharge process of the downward leader channel, showing (a) physical model and (b) electrical equivalent circuit.

A certain time period is needed to collect the charge carriers and the thermal ionization to form a new section of the return stroke. Therefore, in this case, the traveling velocity (v) is less than the speed of light (c).

2.3 Summary

The return stroke process consists of the initial connecting leader process and the subsequent discharge process of the downward leader channel. In the electrical equivalent circuit, both processes can be represented by a current source traveling from the ground in the direction of the thundercloud with the return stroke velocity (v). Therefore, in the TCS model, it is not necessary to distinguish between both processes.

3. Current on the return stroke channel

Figure 3 shows the basic assumptions of the TCS model: The return stroke channel is perpendicular to the earth's surface, and it increases in the z-direction with constant return stroke velocity (v). The return stroke channel is considered as an (ideal) transmission line where the current pulses propagate with the speed of light (c). The ground is taken into account by an ideal-conducting plane.

The current (i_Q) is injected at the top of the return stroke channel from the current source, which begins to travel at $t = 0$ from ground level. When injected current arrives at the ground, a fraction of the current is reflected depending on the ground resistance. The reflected current moves up, and it is reflected again at the end of the lightning channel.

The current reflections are considered by the ground reflection coefficient ρ and the top reflection coefficient R. The current at the altitude z, $i(z, t)$, is composed by

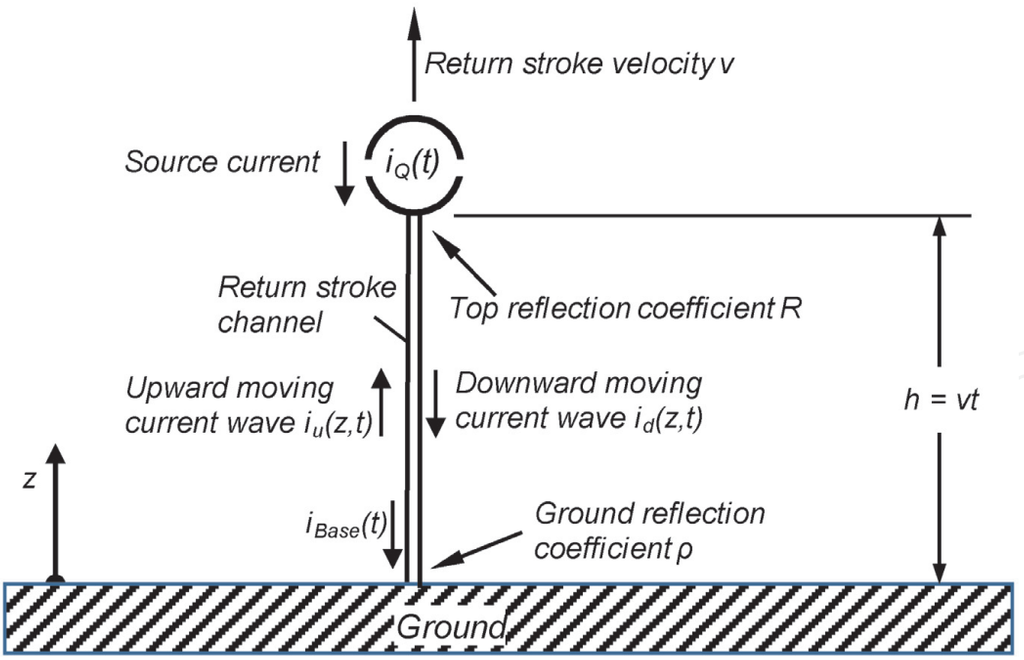

Figure 3
Current distribution on the return stroke channel.

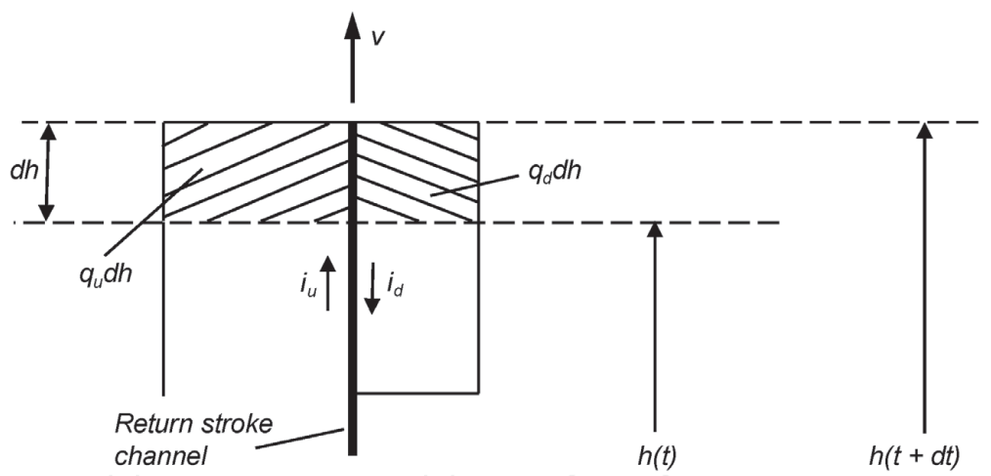

Figure 4.
Current reflection at the upper end of the return stroke channel.

the downward moving current wave $i_d(z, t)$ and the upward-moving current wave $i_u(z, t)$.

3.1 Top reflection coefficient R

Figure 4 shows the upward-moving current wave i_u arrives at the channel top (at the height h). The current wave is reflected at the open end of the lightning channel. For the current refection, the reflection point moves with the return stroke velocity $v = dh/dt$ [13].

The increasing lightning channel creates the new channel segment dh during the time interval dt. The new channel segment is loaded by the charge dQ, composed of the charge of the upward moving current wave (i_u) and the downward moving current wave (i_d). The charge density of the upward moving wave (q_u) and the downward-moving wave (q_d) is given by (c: speed of light):

$$q_u = \frac{i_u}{c} \tag{3}$$

$$q_d = -\frac{i_d}{c} \tag{4}$$

In Eq. (4), the negative sign is due to the current propagation in the opposite direction compared to the coordinate z. The charge dQ is given by:

$$dQ = q_u dh + q_d dh \tag{5}$$

Hence follows:

$$i = \frac{dQ}{dt} = q_u \frac{dh}{dt} + q_d \frac{dh}{dt} = q_u v + q_d v = i_u \frac{v}{c} - i_d \frac{v}{c} \tag{6}$$

The current is given by:

$$i = i_u + i_d \tag{7}$$

With Eqs. (6) and (7), the top reflection coefficient results in:

$$R = \frac{i_d}{i_u} = -\frac{c - v}{c + v} = -A \tag{8}$$

For example, if we assume the return stroke velocity $v = c/3 = 100$ m/μs, the top reflection coefficient is $R = -0.5$, i.e. the half of the current is reflected.

3.2 Source current i_Q and channel base current i_{Base}

The TCS model uses the source current (i_Q) as the input parameter. Because current data are only available from measurements at the striking point, converting the cannel-base current (i_{Base}) into the source current (i_Q) is required. This conversion is deduced in the following.

The channel-base current (i_{Base}) is composed of the downward-moving current wave ($i_{Base/d}$) and the upward-moving current wave ($i_{Base/u}$). With $i_{Base/u} = \rho \cdot i_{Base/d}$, it follows:

$$i_{Base} = i_{Base/u} + i_{Base/d} = (1 + \rho) i_{Base/d} = \frac{1 + \rho}{\rho} i_{Base/u} \tag{9}$$

The reflected current component $\rho \cdot i_{Base/d}(t)$ arrives at the top of the lightning channel after the delay time T. Because at the time $(t + T)$, the distance of propagation cT is equal to the height of the lightning channel $h = v\ (t + T)$, the delay time T can be written as:

$$T = \frac{v}{c - v} t \tag{10}$$

After the reflection at the upper end of the lightning channel, the (reflected) current wave $R\rho \cdot i_{Base/d}(t)$ moves down. The total downward moving current wave $i_d(h, t + T)$ is composed of this reflected current wave and the current from the current source $i_Q(t)$. This current wave arrives at the ground after the delay time T.

At ground level, the downward moving current wave is given by:

$$i_{Base/d}(t+2T) = i_Q(t+T) + R\rho \cdot i_{Base/d}(t) \tag{11}$$

With Eqs. (8) and (10), it follows:

$$(t+2T) = \frac{t}{A} \tag{12}$$

$$(t+T) = \frac{t}{Ak} \tag{13}$$

The coefficient k is:

$$k = 1 + \frac{v}{c} \tag{14}$$

Thus, Eq. (11) can be rewritten as:

$$i_{Base/d}\left(\frac{t}{A}\right) - R\rho \cdot i_{Base/d}(t) = i_Q\left(\frac{t}{Ak}\right) \tag{15}$$

Substituting the time t/A by the time t, it further follows:

$$i_{Base/d}(t) - R\rho \cdot i_{Base/d}(At) = i_Q\left(\frac{t}{k}\right) \tag{16}$$

Now, the following iterative procedure is applied to Eq. (16). Between each iteration step, the equation is multiplied by the factor $(R\rho)$ and the time is multiplied by the factor A resulting in the times A^1t, A^2t, A^3t ...:

$$R^1\rho^1 i_{Base/d}\left(A^1t\right) - R^2\rho^2 \cdot i_{Base/d}\left(A^2t\right) = R^1\rho^1 i_Q\left(\frac{t}{k}A^1\right) \tag{17}$$

$$R^2\rho^2 i_{Base/d}\left(A^2t\right) - R^3\rho^3 \cdot i_{Base/d}\left(A^3t\right) = R^2\rho^2 i_Q\left(\frac{t}{k}A^2\right) \tag{18}$$

$$R^3\rho^3 i_{Base/d}\left(A^3t\right) - R^4\rho^4 \cdot i_{Base/d}\left(A^4t\right) = R^3\rho^3 i_Q\left(\frac{t}{k}A^3\right) \tag{19}$$

The addition of the series of equations gives the following formula:

$$i_{Base/d}(t) = \sum_{\nu=0}^{\infty} (R\rho)^\nu \cdot i_Q\left(\frac{t}{k}A^\nu\right) \tag{20}$$

Substituting the time t by the time kt, Eq. (20) can be rewritten:

$$i_{Base/d}(kt) = i_Q(t) + R\rho \cdot i_Q(At) + \sum_{\nu=2}^{\infty} (R\rho)^\nu i_Q(A^\nu t) \tag{21}$$

Now, Eq. (21) is multiplied by the factor $(-R\rho)$, and the time t is substituted by the time At. It results:

$$-R\rho \cdot i_{Base/d}(Akt) = -R\rho \cdot i_Q(At) - R\rho \cdot \sum_{\nu=1}^{\infty} (R\rho)^\nu i_Q\left(A^{\nu+1}t\right) \tag{22}$$

and from it

$$-R\rho \cdot i_{Base/d}(Akt) = -R\rho \cdot i_Q(At) - \sum_{\nu=2}^{\infty} (R\rho)^\nu i_Q(A^\nu t) \tag{23}$$

From adding Eqs. (21) and (23), it follows:

$$i_Q(t) = i_{Base/d}(kt) - R\rho \cdot i_{Base/d}(Akt) \tag{24}$$

With Eqs. (9) and (24), the source current can be rewritten as a function of the channel-base current:

$$i_Q(t) = \frac{1}{1+\rho}\left[i_{Base}(kt) - R\rho \cdot i_{Base}(Akt)\right] \tag{25}$$

With Eqs. (9) and (21), the channel-base current can be rewritten as a function of the source current:

$$i_{Base}(t) = (1+\rho)\sum_{\nu=0}^{\infty}(R\rho)^{\nu} i_Q\left(\frac{t}{k}A^{\nu}\right) \tag{26}$$

Eqs. (25) and (26) are the fundamental equations of the TCS model. They provide the source current $i_Q(t)$ conversion into the channel-base current $i_{Base}(t)$ and vice versa.

3.3 Lightning current along return stroke channel

When the downward propagating current wave, $i_d(z, t)$, starts from the height z, it arrives at the ground after the time delay z/c. With Eq. (9), it follows:

$$i_d(z,t) = i_{Base/d}(t + z/c) = \frac{1}{1+\rho} i_{Base}(t + z/c) \tag{27}$$

In the opposite case, when an upward-moving current starts at the time (t-z/c) from ground level (z = 0), it arrives at time t at the height z. With Eq. (9), it follows:

$$i_u(z,t) = i_{Base/u}(t - z/c) = \frac{\rho}{1+\rho} i_{Base}(t - z/c) \tag{28}$$

From adding Eqs. (27) and (28), the total current results:

$$i(z,t) = \frac{1}{1+\rho}\left[\, i_{Base}\left(t + \frac{z}{c}\right) + \rho \cdot i_{Base}\left(t - \frac{z}{c}\right)\right] \tag{29}$$

At the upper end of the return stroke channel ($z = h$), the current is given by:

$$i(h,t) = \frac{1}{1+\rho}\left[\, i_{Base}\left(t + \frac{h}{c}\right) + \rho \cdot i_{Base}\left(t - \frac{h}{c}\right)\right] \tag{30}$$

With the channel height $h = vt$, it follows:

$$i(h,t) = \frac{1}{1+\rho}\left[\, i_{Base}(kt) + \rho \cdot i_{Base}(Akt)\right] \tag{31}$$

3.4 Special case of no ground reflections

The reflections at the ground are often ignored, and the ground reflection coefficient is set to ρ = 0. In this case, the relation between the current along the

lightning channel and the channel-base current can be simplified. From Eq. (29), it results for $z \leq h$:

$$i(z,t) = i_{Base}\left(t + \frac{z}{c}\right) \tag{32}$$

From Eq. (25), the relation between the source current (i_Q) and the channel-base current (i_{Base}) follows to:

$$i_Q(t) = i_{Base}(kt) \tag{33}$$

4. Electric and magnetic fields

Figure 5 shows the situation when an electric and magnetic field component is emitted from the infinitesimal small element *dz* located at the lightning channel in the height *z*. The field emitted from the lightning channel arrives after the time interval *r/c* at the point X in the distance *s*. Thus, the retarded time t_x is introduced to consider the propagation time:

$$t_x = t - \frac{r}{c} = t - \frac{\sqrt{s^2 + z^2}}{c} \tag{34}$$

For an observer in point *X*, the apparent height of the lightning channel is $h_x = vt_x$ (v = const.). Using $z = h_x$ in Eq. (34), the apparent height follows to [14]:

$$h_x(t) = \frac{v}{c^2 - v^2}\left(c^2 t - \sqrt{v^2 c^2 t^2 + c^2 s^2 - v^2 s^2}\right) \tag{35}$$

The differentiation by time provides the apparent return stroke velocity [14]:

$$v_x(t) = \frac{dh_x(t)}{dt} = \frac{v}{1 - \frac{v^2}{c^2}}\left(1 - \frac{v^2 t}{\sqrt{v^2 c^2 t^2 + c^2 s^2 - v^2 s^2}}\right) \tag{36}$$

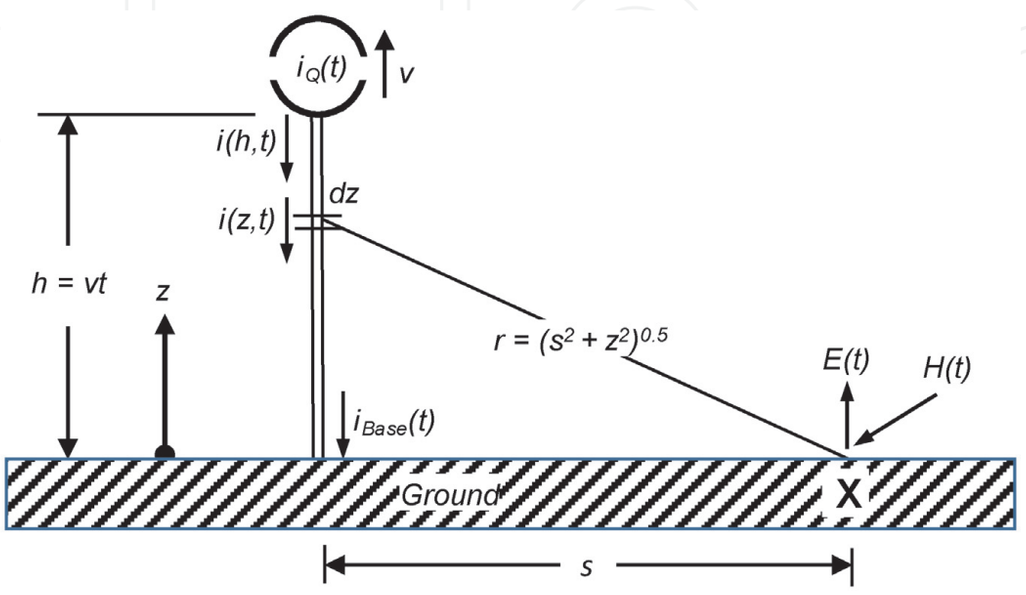

Figure 5.
Field emission from the return stroke channel.

The electric field is perpendicular to the earth's surface. With the apparent height h_x and the retarded time t_x, the vertical electric field in the distance s is given by [14, 15]:

$$E(t) = E_Q(t) + E_i(t) + E_{di}(t) + \Delta E(t) \tag{37}$$

The first term (E_Q) represents the electrostatic field, the second term (E_i) the intermediate field, and the third term (E_{di}) the radiation field. The terms are given by (ε_0 = 8.854 F/m):

$$E_Q(t) = \frac{1}{2\pi\varepsilon_0}\int_0^{h_x}\frac{s^2-2z^2}{r^5}\left(\int_{t_{x/0}}^{t_x} i(z,\tau)d\tau\right)dz \tag{38}$$

$$E_i(t) = \frac{1}{2\pi\varepsilon_0}\int_0^{h_x}\frac{s^2-2z^2}{cr^4}i(z,t_x)dz \tag{39}$$

$$E_{di}(t) = \frac{1}{2\pi\varepsilon_0}\int_0^{h_x}\frac{s^2}{c^2r^3}\frac{\partial i(z,t_x)}{\partial t}dz \tag{40}$$

In Eq. (38), the lower constant of integration $t_{x/0}$ denotes the retarded time when the tip of the lightning channel arrived at the height z. The magnetic field is horizontal to the earth's surface. The horizontal magnetic field is given by [14, 15]:

$$H(t) = H_i(t) + H_{di}(t) + \Delta H(t) \tag{41}$$

The first term (H_i) represents the induction field, and the second term (H_{di}) the radiation field. The terms are given by:

$$H_i(t) = \frac{1}{2\pi}\int_0^{h_x}\frac{s}{r^3}i(z,t_x)dz \tag{42}$$

$$H_{di}(t) = \frac{1}{2\pi}\int_0^{h_x}\frac{s}{cr^2}\frac{\partial i(z,t_x)}{\partial t}dz \tag{43}$$

From **Figure 4**, it can be seen that the current changes abruptly at the upper end of the lightning channel. The abrupt current change represents a discontinuity at the open end of a transmission line. The discontinuity moves upwards with the return stroke velocity $v = dh/dt$, i.e., the current $i(h, t)$ is turned on at the channel segment dh during the time interval dt. This is taken into account by the following term:

$$\frac{\partial i(h,t)}{\partial t}dh = \frac{\partial h}{\partial t}di = -v\cdot di \tag{44}$$

The negative value indicates that the propagation of the current is in the opposite direction compared to the coordinate z. The abrupt current change is responsible for the additional far field terms $\Delta E(t)$ and $\Delta H(t)$ in Eq. (37) and in Eq. (41). These terms are often referred to in the literature as turn-on terms [16].

Of course, for an observer in the distance s, the real height has to be substituted by the apparent height h_x and the real return stroke velocity by the apparent return stroke velocity v_x.

The turn-on terms are finally given by [14]:

$$\begin{aligned}\Delta E(t) &= \frac{1}{2\pi\varepsilon_0}\int_{h_{x,-}}^{h_{x,+}} \frac{s^2}{c^2 r^3}\frac{\partial i(z,t_x)}{\partial t}dh_x \\ &= > \Delta E(t) = \frac{1}{2\pi\varepsilon_0}\frac{s^2}{c^2\left(\sqrt{s^2+h_x^2}\right)^3}v_x \cdot i(h_x,t_x)\end{aligned} \tag{45}$$

$$\begin{aligned}\Delta H(t) &= \frac{1}{2\pi}\int_{h_{x,-}}^{h_{x,+}} \frac{s}{cr^2}\frac{\partial i(z,t_x)}{\partial t}dh_x \\ &= > \Delta H(t) = \frac{1}{2\pi}\frac{s}{c\left(s^2+h_x^2\right)}v_x \cdot i(h_x,t_x)\end{aligned} \tag{46}$$

5. Examples

The waveform of the electric and magnetic fields is well-known from measurements at various distances. According to the distance, the field is usually classified into three groups: near field, intermediate field, and far field. The near field distance range is up to several kilometers, the intermediate field distance range is from several kilometers up to several tens of kilometers, and the far field distance range is from several tens of kilometers up to several hundreds of kilometers.

The basic features are as follows [17]:

- The electric and magnetic field exhibits an Initial Peak at distances of more than several hundred meters.
- The near electric field exhibits a Ramp (up to the maximum) after the Initial Peak,
- The near magnetic field exhibits a Hump after the Initial Peak,
- The electric and magnetic far field exhibits a Zero Crossing after the Initial Peak.

The following shows, by using two examples, that the TCS model reproduces these basic features.

The first example analyses the influence of the ground reflection on the current and on the electric and magnetic field for a typical negative first return stroke at a near distance. The second example presents the electric and magnetic field for a typical subsequent return stroke at a near, intermediate, and far distance. In both examples, the return stroke velocity is chosen to $v = c/3 = 100\ m/\mu s$. The following predefined source current is used (For example, see [12]):

$$i_Q(t) = \frac{i_{Q/max}}{\eta}\cdot\frac{\left(\frac{t}{\tau_1}\right)^m}{1+\left(\frac{t}{\tau_1}\right)^m}\cdot e^{t/\tau_2} \tag{47}$$

The coefficient η denotes the correction factor for the current maximum. The coefficients τ_1 and τ_1 are the front and decay time parameters of the current waveform.

5.1 Influence of ground reflection

In Eq. (47), the current parameters are chosen to $i_{Q/max}$ = 30 kA, m = 5, τ_1 = 1.26 μs and τ_2 = 56.3 μs. The maximum current steepness (di_Q/dt_{max}) is about 32 $kA/\mu s$. These values are typical for a negative first return stroke [18, 19].

The characteristic impedance of the lightning channel is about 1000 Ω [20]. The grounding resistance of poorly grounded buildings is often in the same order of magnitude. In this case, the ground reflection can be neglected. On the other hand, the current ground reflections cannot be ignored when well-grounded structures have much lower resistances. For instance, the well-grounded Peissenberg tower has a ground reflection coefficient of about ρ = 0.7 [21].

In the following, the two cases are analyzed, i.e., the ground reflection coefficient is set to ρ = 0 and ρ = 0.7. **Figure 6a** and **b** show the influence of the ground reflection on the channel-base currents (i_{Base}) (at the striking point). For ρ = 0, the peak current is identical with the peak value of the source current, $i_{Q/max}$ = 30 kA. For ρ = 0.7, the peak current is 43.5 kA, equating to an increase of 45%. **Figure 6c** shows, that the maximum current steepness also got higher by 65.6%, from 24.1 $kA/\mu s$ for ρ = 0 to 39.9 $kA/\mu s$ for ρ = 0.7. The 10–90% rise time decreased accordingly, from $T_{10–90\%} \approx 1.4\ \mu s$ for ρ = 0 to $T_{10–90\%} \approx 1.1\ \mu s$ for ρ = 0.7.

Figures 7 and **8** show the corresponding electric and magnetic fields in a distance of 3 km. The measured Initial Peak of the electric field (E_{max}) and magnetic field (H_{max}) is successfully reproduced, but it is more pronounced for ρ = 0.7, i.e., the initial field peak is about 44% higher for ρ = 0.7 compared to ρ = 0.

The electric field exhibits the Ramp (**Figure 7a**), and the magnetic field exhibits the Hump (**Figure 8a**), known from measurements. The Ramp and Hump are more pronounced for ρ = 0.7 compared to ρ = 0. The different steepness of the Ramp is due to the current reflections, but the final value of the electric field is the same (not shown here) because the total charge transfer is unaltered.

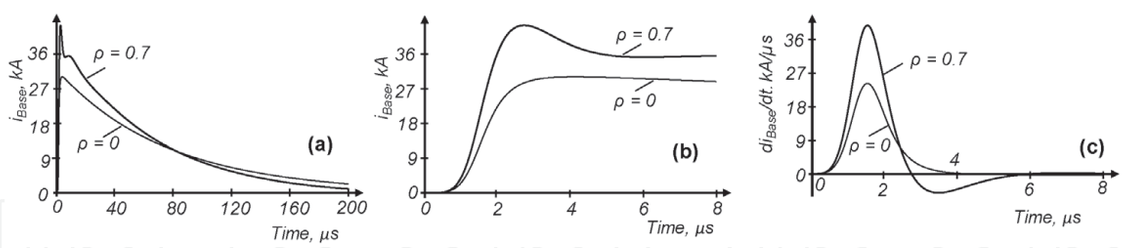

Figure 6.
Channel-base current as a function of the ground reflection factor ρ, showing (a) the total current, (b) the current front, and (c) the current derivative.

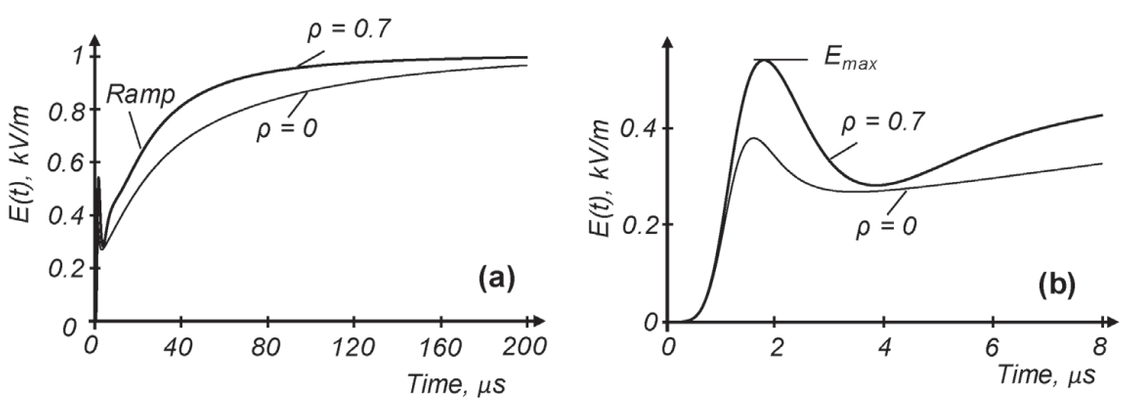

Figure 7.
Electric field in 3 km *distance, showing (a) total field and (b) field front.*

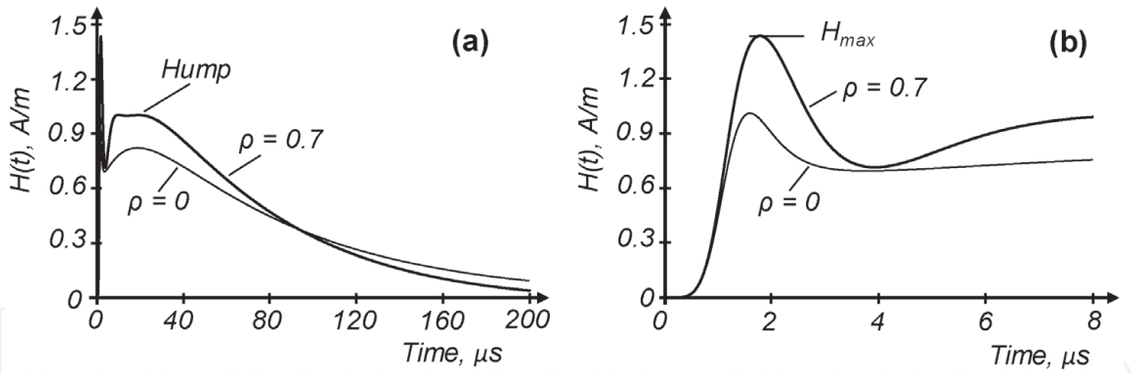

Figure 8.
Magnetic field in 3 km distance, showing (a) total field and (b) field front.

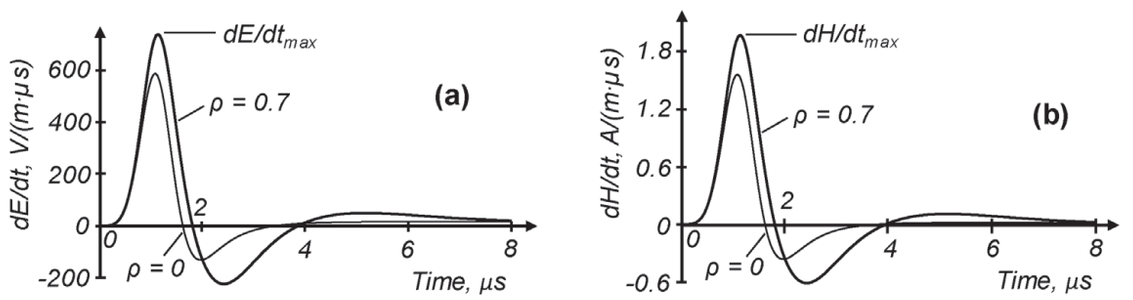

Figure 9
Derivative of (a) Electric field and (b) magnetic field in 3 km *distance.*

Figure 9 shows that the influence of the current reflections on the field derivative is comparably low. For $\rho = 0.7$, the maximum of the electric and magnetic field derivative (dE/dt_{max}, dH/dt_{max}) is about 26% higher, and the full width at half maximum ($FWHM$) is higher by less than 20%.

5.2 Electric and magnetic field at near, intermediate, and far distance

In Eq. (47), the current parameters are chosen to $i_{Q/max} = 10\,kA$, $m = 4$, $\tau_1 = 0.7\,\mu s$ and $\tau_2 = 30\,\mu s$. Ground reflection is ignored ($\rho = 0$) and the return stroke velocity is chosen to $100\,m/\mu s$. For the channel-base current (i_{Base}) (at the striking point), the peak value is $10\,kA$, the 10–90% rise time is $0.94\,\mu s$ and the time to half value is $31\,\mu s$. These values are typical for subsequent return strokes [18, 19, 22].

Figure 10 shows the electric and magnetic fields at $1\,km$ (near field), $10\,km$ (intermediate field), and $100\,km$ (far field). It can be seen that the main characteristics of the electric and magnetic fields are reproduced with the TCS model, i.e., the Initial Peak of the electric and magnetic field, the Ramp of the near electric field, the Hump of the near magnetic field, and the Zero Crossing of the electric and magnetic far field.

At far distances, the electric and magnetic field is approximately given by the radiation term (E_{di}, H_{di}) according to Eqs. (40) and (43). In this case, the electromagnetic field (E_{far}, H_{far}) has a behavior like a plane wave in free space, given by the following formula (Compare [6]):

$$\frac{E_{far}}{H_{far}} = c \cdot \mu_0 = \Gamma_0 \tag{48}$$

$\mu_0 = 4\pi \cdot 10^{-7}\,H/m$: Permeability of free space.
$\Gamma_0 = \pi \cdot 120\,\Omega \approx 377\,\Omega$: Impedance of free space.

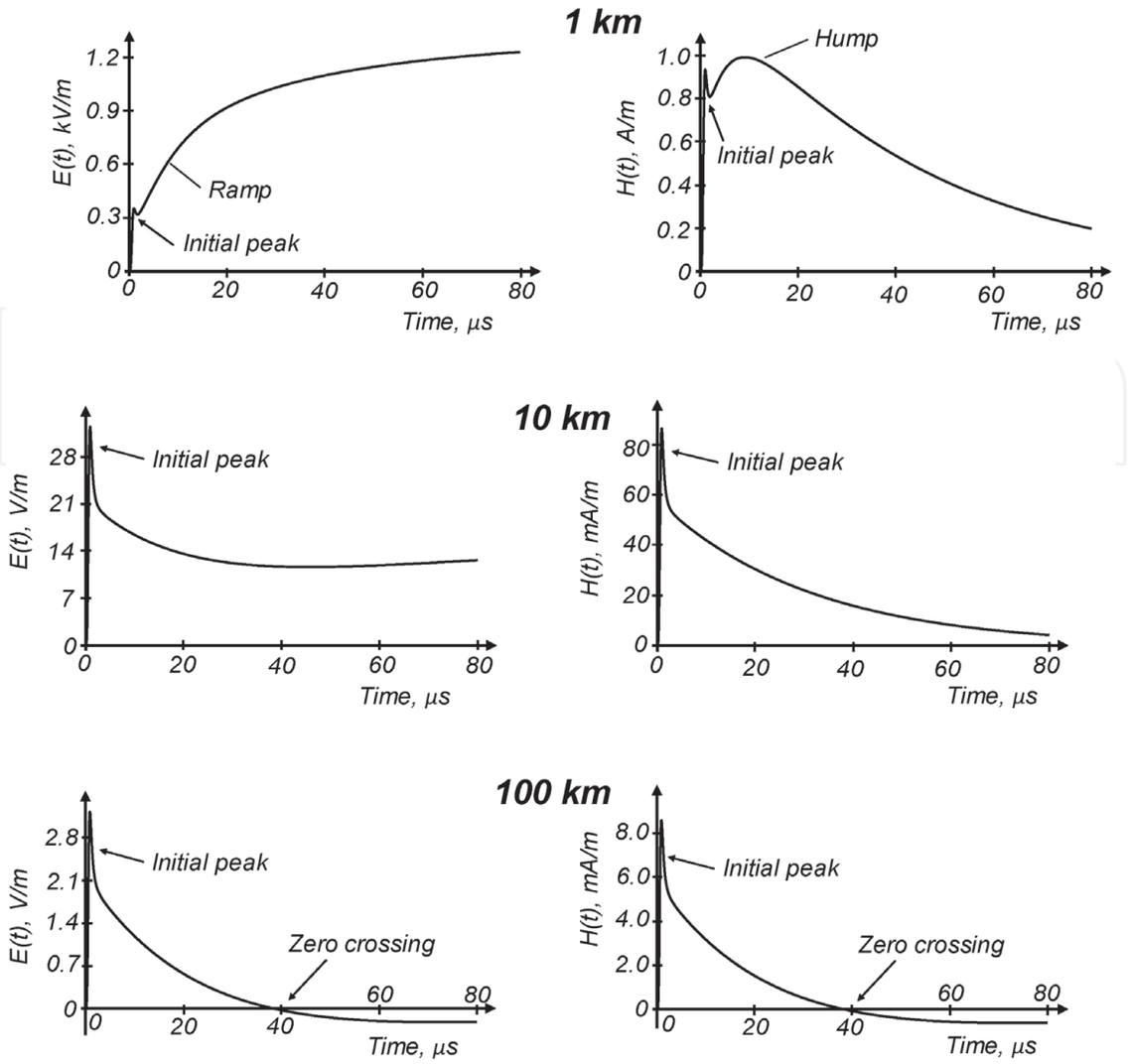

Figure 10.
Electric field, E(t)*, and magnetic field,* H(t)*, of a subsequent return stroke in the distances of 1, 10, and 100* km*. For the channel-base current (at the striking point), the peak current, 10* kA*, rise time, 0.94* μs*, and time to half value, 31* μs*.*

As shown in Eq. (48), the electric and the magnetic far fields are linked together by the impedance of free space. Therefore, the waveform of the electric and magnetic fields is the same at far distances, as shown in **Figure 10**.

At 100 *km*, the Initial Peak of the electric field is 3.2 *V/m*, which agrees very well with measured data that varies between 2.7 and 5.0 *V/m* [5].

5.3 Summery

The examples show that the main features of the measured electric and magnetic fields are reproduced with the TCS model. These are the Ramp of the near electric field, Hump of the near magnetic field, Zero Crossing of the far distant electric and magnetic fields, and Initial Peak of the electric and magnetic fields for near, intermediate, and far distances.

DOI: http://dx.doi.org/10.5772/intechopen.98898

Author details

Fridolin Heidler
University of the Federal Armed Forces Munich, Neubiberg, Germany

*Address all correspondence to: fridolin.heidler@unibw.de

References

[1] IEC 62305-1. Protection against lightning-Part 1: General principles. 2nd ed. Geneva: IEC; 2010.

[2] IEC 62305-3. Protection against lightning-Part 3: Physical damages and life hazard. 2nd ed. Geneva: IEC; 2010.

[3] Habiger E. Electromagnetic compatibility. 1st ed. Heidelberg: Hueting;1992.

[4] IEC 62305-4. Protection against lightning-Part 4: Electrical and electronic systems within structures. 2nd ed. Geneva: IEC; 2010.

[5] Rakov V, Uman M. Lightning: Physics and Effects. 1st ed. New York: Cambridge Univ. Press; 2003.

[6] Uman M, McLain D, Krider E. The electromagnetic radiation from a finite antenna. Am. J. Phys. 1975; 43:33-38.

[7] Uman M, McLain D. Magnetic field of lightning return stroke. J. Geophysical Res. 1969; 74:6899-6910.

[8] Bruce C, Golde R. "The Lightning Discharge," J. Institution of Electrical Engineers. 1941; 88:6:487-505.

[9] Nucci C, Mazzetti C, Rachidi F, Ianoz M. On lightning return stroke models for LEMP calculations. In: Proceedings of the 19th Intern. Conf. on Lightning Protection (ICLP '88); 25-29 April; Graz, Austria; 1988: p. 463-470.

[10] Rakov V, Dulzon A. A modified transmission line model for lightning return stroke field calculation. In: Proceedings of the 9th Intern. Zurich Symposium on Electromagnetic Compatibility (EMC '91); 12-14 March1991; Zurich, Switzerland; 1991: p. 229-234.

[11] Heidler F. Traveling current source model for LEMP calculation. In: Proceedings of the 6th Intern. Symposium on Electromagnetic Compatibility (EMC '85); 5-7 March 1985; Zurich, Switzerland; 1985: p.157-162.

[12] Heidler F. Review and extension of the TCS model to consider the current reflections at ground and at the upper end of the lightning channel. IEEE Trans. on EMC. 2019; 61:3:644-652. DOI: 10.1109/TEMC.2018.2890342

[13] Heidler F, Hopf C. Influence of the lightning channel termination on the lightning current and lightning electromagnetic impulse. In: Proceedings of the 16th International Aerospace and Ground Conference on Lightning and Static Electricity (ICOLSE '94); 24-27 May 1994; Mannheim, Germany; 1994: p. 65-74.

[14] Heidler F, Hopf C. Lightning current and lightning electromagnetic impulse considering current reflection at the earth's surface. In: Proceedings of the 22nd International Conference on Lightning Protection (ICLP'94); Budapest, Hungary;1994: report R 4-05.

[15] Rakov V, Uman A. Review and evaluation of lightning return stroke models including some aspects of their application. IEEE-Trans. on EMC. 1998; 40:4,403-426. DOI: 10.1109/15.736202.

[16] Rachidi F. The quandary of direct measurement and indirect estimation of lightning current parameters. In: Proceedings of the 27th International Conference on Lightning Protection (ICLP '04); Avignon, France; 2004: p. 36-51.

[17] Lin Y, Uman M, Tiller J, Brantley R, Beasley W, Weidman C. Characterization of lightning return stroke electric and magnetic fields from simultaneous two-station measurements. Journal of Geophysical Research. 1979; 84:C10:6307-6314.

[18] Berger K, Anderson R, Kroeninger H. Parameters of lightning flashes. Electra. 1975; 41:23-37.

[19] Anderson R, Eriksson A. Lightning parameters for engineering application. Electra. 1980; 69:65-102.

[20] Trapp N. Measurement of the current waveform and the current parameters with automatically operating lightning current measuring stations. PhD. Munich: Technical University Munich; 1985; translation from German.

[21] Fuchs F. On the transient behavior of the telecommunication tower at the mountain Hoher Peissenberg. In: Proceedings of the 27th International Conference on Lightning Protection (ICLP `98); Birmingham, UK; 1998: p. 36-41.

[22] Heidler F, Paul Ch. Some return stroke characteristics of negative lightning flashes recorded at the Peissenberg Tower. IEEE-Trans. on EMC. 2017; 59:5,1490-1497. DOI: 10.1109/TEMC.2017.2688587